NASA Technical Paper 1061

Vapor Ingestion in Centaur Liquid-Hydrogen Tank

Eugene P. Symons

OCTOBER 1977

NASA

NASA Technical Paper 1061

Vapor Ingestion in Centaur Liquid-Hydrogen Tank

Eugene P. Symons
Lewis Research Center
Cleveland, Ohio

National Aeronautics
and Space Administration

**Scientific and Technical
Information Office**

1977

VAPOR INGESTION IN CENTAUR LIQUID-HYDROGEN TANK

by Eugene P. Symons

Lewis Research Center

SUMMARY

An experimental investigation of the vapor-ingestion phenomena, as it occurs in the Centaur liquid-hydrogen tank was conducted. The equations presented herein can be used to predict the anticipated fluid height above the tank outlet at which vapor ingestion may be expected to initiate as a function of the dimensionless grouping $W/(1 + B)$, where W is the outflow Weber number and B is the Bond number. Experiment data were obtained in small-scale Centaur liquid-hydrogen tanks at normal gravity and compared with predicted results. The overall agreement of analysis and experiment is very good. Additionally, predictions of minimum liquid hydrogen levels required to prevent vapor ingestion when restarting the engines in space and the quantities of liquid remaining in the tank at vapor ingestion during main engine firing are presented.

INTRODUCTION

The Lewis Research Center has been studying the phenomena that occur during liquid outflow from various tank systems. Earlier studies (refs. 1 and 2) examined the distortion of the liquid-vapor interface during the draining of a cylindrical tank in a weightless environment. More recent studies have examined the vapor-ingestion phenomena in cylindrical containers having both flat (ref. 3) and hemispherical (ref. 4) bottoms. Data from these studies were obtained both in normal gravity and in weightlessness. Other investigations have examined the effectiveness of various baffles (refs. 5 and 6) and the use of outflow rate throttling (ref. 7) as means of reducing liquid residuals (the quantity of liquid remaining in the tank when vapor enters the outlet line) in a low gravity environment.

This report presents the results of an experimental study of the vapor-ingestion phenomena as it occurs in a scale model of the Centaur liquid-hydrogen tank. The objective was to experimentally determine the height of the liquid free surface in the tank

when vapor is initially ingested into the tank outlet. These data and those obtained previously in reference 8 could then be compared with an approximate analysis (ref. 9), which predicts the vapor-ingestion height as a function of Weber and Bond number. If the data show that the analysis is valid, the analysis can then be used to predict the depth of liquid in the Centaur tank above which a successful restart of the vehicle engines could be accomplished without the ingestion of vapor resulting in pump cavitation and subsequent loss in engine performance.

In the selection of the tank model and test liquids used in this investigation, some attempt was made to simulate the Bond numbers and Weber numbers that would exist during a typical Centaur engine restart sequence. This resulted in tanks having inside diameters of 8, 15, and 30 centimeters and two test liquids, trichlorotrifluoroethane and ethanol. All tests were performed in normal gravity.

SYMBOLS

A	area, cm^2
a	radius of tank, cm
B	Bond number, $\rho ga^2/\sigma$
b	height of bulkhead, cm
d/h_0	dimensionless distance
F	Froude number, $Q^2/\pi^2 ga^5$
f	dimensionless function
f	denotes function of
g	acceleration, cm/sec^2
H	dimensionless free-surface height, h/b
h	height of free surface above base plane, cm
J	surface curvature, cm^{-1}
K	constant
$\hat{K}$	unit vector normal to surface
p	pressure, N/cm^2
Q	volumetric flow rate, cm^3/sec
R	radius, cm

r	radial coordinate
$\hat{r}$	unit vector in r direction
S	length, cm
u	fluid velocity, cm/sec
W	Weber number, $\rho Q^2/\pi^2\sigma a^3$
Z	axial coordinate
$\hat{Z}$	unit vector in Z direction
β	specific surface tension, σ/ρ, cm^3/sec^2
θ	angular coordinate
$\hat{\theta}$	unit vector in angular direction
μ	liquid viscosity, g/m·sec
ρ	liquid density, g/cm^3
σ	liquid surface tension, N/cm
φ	function

Subscripts:

m	denotes maximum
min	denotes minimum
0	denotes point immediately above outlet
∞	denotes point far from outlet
1, 2	denote principle local radii of curvature

ANALYSIS

In reference 9 Klavins presents an analysis and uses it to predict the vapor ingestion height as a function of the ratio $W/(1 + B)$, where the Weber number W is a dimensionless parameter representing the ratio of inertia to capillary forces and the Bond number B is a dimensionless parameter representing the ratio of gravitational to capillary forces. This specific grouping of parameters was chosen primarily as a result of experiment data (e.g., refs. 3 to 5) which indicate that vapor-ingestion heights tend to correlate with Weber number in weightlessness and with Froude number in normal gravity. It can easily be observed that this grouping does reduce to Weber number in weightlessness (since $B = 0$) and to Froude number in normal gravity (since

$B >> 1$ and W/B = Froude number). This report presents a portion of Klavins' analysis, concentrating on and somewhat amplifying that portion which would be applicable to the restart sequence for a Centaur vehicle (i.e., the high Bond number regime).

Referring to figure 1, we may write Bernoulli's equation for a streamline on the interface between a point far from the drain (∞) and immediately above the drain (0) as

$$p_0 + \rho g h_0 + \frac{1}{2}\rho u_0^2 = p_\infty + \rho g h_\infty \tag{1}$$

Implicit in equation (1) is the assumption that the fluid velocity is negligible at ∞ and that the fluid is inviscid and irrotational.

We may relate the velocity at the point above the drain u_0 to the outflow rate Q by defining a control (or flow) area A into which the influx of fluid will be assumed to be normal and the velocity will be assumed to be uniform and equal to u_0.

Thus we write

$$u_0 A \equiv \int_A \vec{u} \cdot d\vec{A} \cong Q \tag{2}$$

Further, the pressure difference $p_\infty - p_0$ may be related to the surface curvature J.

$$p_\infty - p_0 = -\sigma(J_\infty - J_0) \tag{3}$$

Substituting equations (3) and (2) into equation (1) and introducing the Weber number $W = \rho Q^2/\pi^2\sigma a^3$ and the Bond number $B = \rho g a^2/\sigma$ yield

$$\frac{W}{B}\frac{\pi^2 a^5}{2A^2} = h_\infty - h_0 - \frac{a^2(J_\infty - J_0)}{B} \tag{4}$$

For convenience, the surface curvature term may be replaced by the dimensionless function f, defined as

$$f = -\frac{h_\infty - h_0}{a^2(J_\infty - J_0)} \tag{5}$$

Additionally, since recent studies (ref. 10) indicate that vapor-ingestion data at all acceleration levels can be correlated in terms of the group $W/(1 + B)$, we shall introduce

equation (5) and this group to yield

$$\frac{W}{B+1} = \frac{2}{\pi^2 a^5} \frac{A^2}{f} \left(\frac{1+Bf}{1+B}\right)(h_\infty - h_0) \tag{6}$$

Now we consider equation (6) written in the following form:

$$\frac{W}{B+1} = \frac{2}{\pi^2 a^5} A^2 (h_\infty - h_0) \left[\frac{\frac{1}{f} + B}{1+B}\right] \tag{6a}$$

Making use of this form and noting the typical Bond numbers that occur during the operation of Centaur (i.e., $400 < B_0 < 2\times10^6$), it can be seen that the bracketed term will be of the order of unity for all but extremely small values of the surface curvature function.

Now, as vapor ingestion becomes imminent, h_0 decreases much more rapidly than does h_∞. We can use this fact by differentiating equation (6) with respect to h_0 and then letting $dh_\infty/dh_0 \to 0$. The resulting equation is

$$h_\infty - h_0 = \left[\frac{2}{A}\frac{\partial A}{\partial h_0} - \frac{1}{(Bf+1)}\left(\frac{1}{f}\right)\frac{\partial f}{\partial h_0}\right]^{-1} \tag{7}$$

We may now combine equations (6) and (7) to eliminate h_∞ and provide a relation between $W/(1+B)$ and the bulk liquid depth above the outlet with Bond number as a parameter:

$$\frac{W}{B+1} = \frac{2}{\pi^2 a^5} \frac{A^2}{f}\left(\frac{1+Bf}{1+B}\right)\left[\frac{2}{A}\frac{\partial A}{dh_0} - \left(\frac{1}{Bf+1}\right)\left(\frac{1}{f}\right)\frac{\partial f}{\partial h_0}\right]^{-1}$$

As mentioned in reference 9 the results are applicable to any tank geometry subject to the assumptions of irrotational, inviscid, quasi-steady flow with the fluid filling the drain end of the tank and in the absence of vortexing. The analysis can be specified to a particular tank geometry through the functions A and f.

The proper choice for the control area function A depends on the liquid level in

the tank as well as the tank geometry. In reference 9 two control area functions were posed for the Centaur liquid-hydrogen tank, one for large liquid levels (i.e., liquid covering the top of the bulkhead) and another for low liquid levels (liquid level below the top of the bulkhead).

Limited experiment data (ref. 8) suggest that, for the Weber and Bond numbers that are to be expected during a typical Centaur engine restart sequence, vapor ingestion will occur at relatively low bulk liquid levels in the tank (below the top of the bulkhead). It is assumed that, at these liquid levels, the velocity field is essentially circumferential and that the control area function can be approximated by two planar surfaces described by equation (8) and derived in the appendix.

$$A = 2ah_0 - ab\left[\left(\frac{h_0}{b}\right)\sqrt{1 - \left(\frac{h_0}{b}\right)^2} + \sin^{-1}\left(\frac{h_0}{b}\right)\right] \tag{8}$$

The expression to be utilized for the surface curvature function f is largely dependent on the contact angle of the liquid on the tank material and the Bond number. At large values of the Bond number, the interface is essentially flat, except very near the tank walls where the liquid contacts the wall. At low Bond numbers and for a zero contact angle, the interface is highly curved. Reference 9 examines four possible forms for the surface curvature function, two for $B \ll 1$ and two for $B \gg 1$, which are dependent on the initial liquid level. During a typical Centaur engine restart sequence, Bond numbers are so large that the interface is essentially flat, and, from the limited available data, bulk liquid levels in the tank at vapor ingestion are low $((h_\infty/b) < 1)$. In this case the liquid-vapor interface is in effect a flat ring with a small depression of depth $h_\infty - h_0$ immediately above the outlet. The surface curvature function f corresponding to these conditions is given in reference 9 as $\pi^2/8$. However, an independent derivation outlined in the appendix yielded

$$f = \frac{1}{4} \tag{9}$$

Substitution of equations (8) and (9) into (6) and (7) yields the vapor-ingestion height as a function of the parameter $W/(1 + B)$.

While it is expected that vapor ingestion in the actual Centaur liquid-hydrogen tank will occur at low liquid levels $((h_\infty/b) < 1)$ in its current operation mode, it is conceivable that future missions could be conducted at lower Bond numbers. This would, in turn, be reflected in greater free-surface heights at vapor ingestion and may give rise to instances in which $(h_\infty/b) > 1$. For these situations different values of the control

area function A and the free-surface curvature function f would be required. The relations given in reference 9 are

$$A = \pi h_0^2 \left[1 - \frac{1}{6}\left(\frac{h_0}{a}\right) - \frac{2}{3}\sqrt{1 - \left(\frac{d}{h_0}\right)^2} \right] \tag{10}$$

where

$$\frac{d}{h_0} = \frac{\sqrt{1 + \left(\frac{h_0}{b}\right)^2 \left(\frac{a^2}{b^2} - 1\right)} - 1}{\left(\frac{h_0}{a}\right)\left(\frac{a^2}{b^2} - 1\right)}$$

and

$$f = \frac{1}{4} \tag{11}$$

The derivations of the preceding functions are presented in the appendix.

Again, substitution of equations (10) and (11) into (6) and (7) would yield the vapor-ingestion height as a function of the parameter $W/(1 + B)$.

COMPUTATIONAL SEQUENCE

The computational sequence described in reference 9 may be used to determine the vapor-ingestion height as a function of $W/(1 + B)$. Basically, this involves choosing a system Bond number and a value of $H_0 = h_0/b$. The appropriate equation for A and the value for f are selected based on the choice of Bond number and H_0. Using these values, A can be determined from equation (8) or (10). (In some cases considered in ref. 9, f is a function of H_0; however, for the range of parameters in this study it is constant.) Next, the derivatives necessary in the computation are approximated. (Actual derivatives could be calculated, but in light of the other approximations the method used in ref. 9 was employed.)

$$\frac{\partial A}{\partial h_0} \approx \frac{100}{b}\left[A(H_0 + 0.01) - A(H_0)\right]$$

and, since f is a constant for our studies,

$$\frac{\partial f}{\partial h_0} = 0$$

The values for the derivatives along with those for $A(H_0)$ and f are then substituted into equation (7) to obtain $h_\infty - h_0$, which also prescribes a value for h_∞/b since h_0/b was selected at the outset. The values of $h_\infty - h_0$, $A(h_0)$, and f are then substituted into equation (6) to obtain the parameter $W/(1 + B)$. In this fashion a plot showing the relation of h_∞/b as a function of $W/(1 + B)$ at a point of vapor ingestion can be constructed. Such a plot is shown in figure 2 for $B = 1000$. The parametric spread for other Bond numbers in the range of interest (i.e., 400 to approximately 2×10^6) is negligible, as was expected from an inspection of equation (6a), and thus the curve for $B = 1000$ could be used for all $B > 400$.

Note in figure 2 that the predicted vapor-ingestion height when using the planer area approach (circumferential flow around the bulkhead, eqs. (8) and (9)) differs from that calculated when using the spherical control area (eqs. (10) and (11)). If the region of interest is $(h_\infty/b) < 1$, it is anticipated that the planer area approach is valid, while for $(h_\infty/b) > 1$, the spherical area approach should apply. However, at values of $(h_\infty/b) \approx 1$, it is not clear which form would be appropriate, and experimental verification would be necessary.

APPARATUS AND PROCEDURE

Experiment Tanks

The experiment investigation used t ee cylindrical tanks. The bottoms and outlets of these tanks were scaled models of th entaur liquid-hydrogen tank, and the internal tank diameters were 8, 15, and 30 cent eters. The tanks were fabricated from cast acrylic plastic that had been polished to provide optical clarity. A flat disk having a diameter of 1 tank radius was positioned 1 tank radius below the pressurant gas inlet port to prevent the direct impingement of the incoming gas onto the liquid-vapor interface during draining. The tank was sealed at the top and bottom with an O-ring and was clamped between two stainless-steel plates by four threaded rods. (A photograph of a typical tank is shown in fig. 3).

Test Liquids

Two liquids, trichlorotrifluoroethane and anhydrous ethanol, were employed in this study. The pertinent properties of these liquids are presented in table I. Both liquids had an essentially 0 static contact angle on the tank material in order to duplicate the static contact angle of the liquid hydrogen on the Centaur tank. A small amount of dye was added to the test liquid to improve the photographic quality. The addition of the dye had no measurable effect on the liquid properties as presented in table I.

Experiment Package

The experiment package shown in figure 4 is a self-contained unit consisting of an experiment tank, a pumping system, a photographic system, a digital clock, and an electrical system to operate the various components. Indirect illumination of the experiment tank is provided by means of a backlighting system which allowed the fluid behavior to be recorded by a high-speed, 16-millimeter, motion-picture camera. The pumping system comprises an air reservoir, the experiment tank, a solenoid valve, and a liquid collection tank. The volume of the air reservoir is much greater than the largest volume of liquid drained from the tank during outflow, so the supply pressure remains essentially constant. Elapsed time during the tests is observed by reading a digital clock having an accuracy of ± 0.01 second. A scale positioned beside the tank provides an indication of the initial liquid height as well as the interface height as a function of time during draining. All the electrical components are operated through the control box and receive their power from rechargable nickel-cadmium cells.

Test Procedure

Before the flow components were assembled, the tank and all flow lines were cleaned in an ultrasonic cleaner to assure that the properties of the test liquids would not be affected by the presence of contaminants. The parts were then rinsed with distilled water and dried in a filtered air dryer. All cleaning was done in the Lewis Zero Gravity Class 10 000 Clean Room (fig. 5). All parts were then assembled and mounted in the experiment package. Liquid was then added to the tank and all flow lines. The system was activated several times to purge all trapped air from the lines and checked for leaks. Draining was accomplished by pressurizing the air reservoir to a predetermined pressure (dependent on desired flow rate). A solenoid valve located downstream of the tank outlet initiated the draining.

Before a test, the tank was filled to the desired level (generally about 1 tank radius above the elliptical bulkhead), the air reservoir was pressurized, and the camera was loaded. The tests were then initiated by remotely activating the electrical control box from a control room of the Zero Gravity Facility. (See fig. 6.)

RESULTS AND DISCUSSION

Comparison of Experiment Data with Analysis

A series of draining tests were performed with three scale models of the Centaur liquid-hydrogen tank (1/38, 1/20, and 1/10 scale) using two test liquids (ethanol and trichlorotrifluoroethane) over a range of outflow rates in a normal gravity environment. System Bond numbers ranged from 1331 to 7805 and outflow Weber numbers from 0.0062 to 35.12. The results obtained are compared with the analytical predictions in figure 7. Below nondimensional vapor-ingestion heights of about 1.1, the data agree very well with the curve generated when utilizing the planer control area; for larger nondimensional vapor-ingestion heights, the spherical control area approach more accurately predicts the draining behavior. The relatively good agreement between analysis and the experiment tends to support the assumptions previously made in determining the control area function. A summary of the data is presented in table II.

In figure 8 data obtained in reference 8 are compared with the analytical predictions. In that study two Centaur scale models of the liquid-hydrogen tank (1/3.67 and 1/38 scale) were used in conjunction with two test liquids (ethanol and water) for draining in a normal gravity environment. Again, predicted vapor-ingestion heights are consistently in agreement with those observed experimentally. As was the case for the experiment data taken in the present study, the data of reference 8 compare very well with the planar area approach for nondimensional heights less than about 1.1. Also plotted in figure 8 is a single data point for a full-scale Centaur liquid-hydrogen tank which was obtained from a normal-gravity engine firing.

Implication of Results

By examining a typical Centaur engine restart sequence and calculating the system Bond and Weber numbers, the analytical curves could be used to determine if the vehicle's engines could be successfully restarted without ingesting vapor into the outlet line. Ingestion of vapor could result in pump cavitation and subsequent loss of engine performance.

A typical engine restart sequence consists of an initial settling of the liquid propellant in a high-Bond-number environment followed by propellant outflow from the tank during feed-line chill down, engine cool down, and finally main-engine start. A summary of the Bond numbers and Weber numbers associated with each phase of propellant outflow is given in table III. It should be noted that the calculated Bond numbers are based on the assumption of a vehicle mass of 18 160 kilograms (40 000 lb).

Such an assumption would generally lead to conservative results, since during a restart it is quite likely that the vehicle mass would be appreciably less than this figure because of the propellants expended during earlier engine burns. The lower initial vehicle mass would be reflected in higher system Bond numbers which, in turn, would give rise to lower values of vapor-ingestion height.

The predicted vapor-ingestion heights for the restart events presented in table III are plotted in figure 9. Of the three events the most critical is the engine cool-down phase. As shown, this results in the largest value of vapor-ingestion height of $h_\infty/b = 0.9$ or, conversely, that an engine restart could not be accomplished without ingesting vapor into the outlet line if the initial liquid level were less than this value.

It should be noted that the same curves could be used to predict the vapor-ingestion height (and, thus, the liquid residuals), which are to be expected during a main engine burn. Since the liquid-vapor interface may be expected to be flat because of the high Bond number, the vapor-ingestion height can be used to compute the volume of liquid remaining in the tank when vapor ingestion occurs. For example, if the Bond number was based on a vehicle mass of 18 160 kilograms (40 000 lb), the corresponding nondimensional vapor-ingestion height can be determined from figure 9 as approximately 0.45. This, in turn, corresponds to liquid residuals of 2.45×10^5 cubic centimeters ($8.65\ ft^3$) or in terms of liquid mass 1.57×10^4 grams (34.6 lbm).

SUMMARY OF RESULTS

An experimental investigation of the vapor ingestion phenomena was conducted in 1/38, 1"20, and 1/10 scale models of the Centaur liquid-hydrogen tank. All tests were performed in a normal-gravity environment with two test liquids, trichlorotrifluoroethane and ethanol, over a range of outflow rates. Bond numbers B (based on the tank radius) ranged from 1331 to 7804, and Weber numbers W ranged from 0.0062 to 35.12. The data obtained from the tests were compared with an approximate analysis of the phenomena which yielded the vapor-ingestion height as a function of the dimensionless grouping $W/(B + 1)$. For dimensionless vapor-ingestion heights (h_∞/b) less than 1.1, the analysis, based on a plane-control area which assumes circumferential flow around the elliptical bulkhead, agreed very well with the experiment data. For larger dimen-

sionless vapor-ingestion heights, the analysis, based on a spherical control area compared well with the data.

Additionally, previously obtained experiment data were compared with the analysis. These data, obtained using both water and ethanol in 1/3.67 and 1/38 scale models of the Centaur liquid-hydrogen tank, again compared very favorably with the analytical model as did one data point obtained from an actual test firing in a full-scale liquid-hydrogen tank.

Utilizing the analysis, it was determined that the Centaur's engines could be successfully restarted after settling without the danger of ingesting vapor into the outlet, provided the initial liquid level in the tank was greater than 90 percent of the height of the bulkhead. The most critical phase of the Cantaur restart sequence was found to be the engine cool-down phase. Additionally, for main engine burn for the actual Centaur vehicle, it was calculated that vapor ingestion would not occur until the liquid volume in the tank had dropped below 2.45×10^5 cubic centimeters (8.65 ft^3).

Lewis Research Center,
National Aeronautics and Space Administration,
Cleveland, Ohio, July 29, 1977,
491-02.

APPENDIX - DETERMINATION OF CONTROL AREA AND SURFACE CURVATURE FUNCTIONS CONTROL AREA FUNCTION

As stated in the text, a proper choice for the control area function A depends on both the liquid level in the tank as well as the tank geometry. In reference 9 two choices were posed for the control area function appropriate for the Centaur liquid-hydrogen tank; one for large liquid levels (i.e., liquid level covering the top of the ellipsoidal bulkhead) and another for low liquid levels (i.e., liquid levels below the top of the ellipsoidal bulkhead).

If the initial liquid level is significantly above the top of the bulkhead, the velocity potential is generally approximated by a point sink, and an appropriate control area would be a spherical surface surrounding the tank drain. Such a control area is indicated in figure 10. Since it is necessary to know the surface area of this control surface for computational purpose, we will first develop a general expression for determining surface areas and then specify that general expression to the Centaur liquid-hydrogen tank.

We first suppose that there exists some arbitrary three-dimensional surface, say $\varphi = \varphi(r, \theta, Z)$ and attempt to find the projection of that surface onto the $r-\theta$ plane.

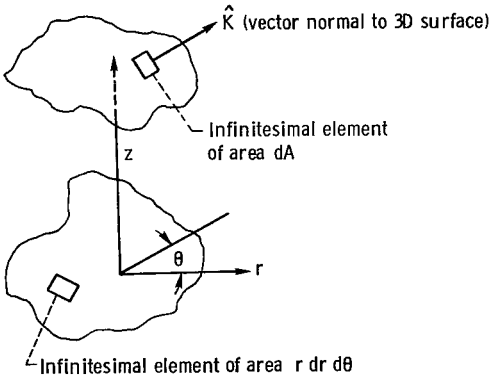

We may then write, in general,

$$dA(\hat{Z} \cdot \hat{K}) = r\, dr\, d\theta \tag{A1}$$

where A is the total surface area of the arbitrary three-dimensional surface, $\hat{K}$ is the unit vector normal to the three-dimensional surface, and $\hat{Z}$ is the unit vector in the Z-direction. Now

$$\hat{K} = \frac{\nabla\varphi}{|\nabla\varphi|} \tag{A2}$$

where φ is the equation describing the three-dimensional surface. And

$$\nabla\varphi = \frac{\partial\varphi}{\partial r}\hat{r} + \frac{1}{r}\frac{\partial\varphi}{\partial\theta}\hat{\theta} + \frac{\partial\varphi}{\partial Z}\hat{Z} \tag{A3}$$

with $\hat{r}$ the unit vector in the r direction and $\hat{\theta}$ the unit vector in the θ direction. Since

$$Z = f(r, \theta)$$

then

$$\varphi = Z - f(r, \theta) \tag{A4}$$

And we can then express equation (A3) as

$$\Delta\varphi = -\frac{\partial f}{\partial r}\hat{r} - \frac{1}{r}\frac{\partial f}{\partial\theta}\hat{\theta} + \hat{Z} \tag{A5}$$

with

$$|\Delta\varphi| = \sqrt{\left(\frac{\partial f}{\partial r}\right)^2 + \frac{1}{r^2}\left(\frac{\partial f}{\partial\theta}\right)^2 + 1} \tag{A6}$$

Combining equations (A5) and (A6) yields

$$\hat{K} = \frac{-\left(\frac{\partial f}{\partial r}\right)\hat{r} - \frac{1}{r}\left(\frac{\partial f}{\partial\theta}\right)\hat{\theta} + \hat{Z}}{\sqrt{\left(\frac{\partial f}{\partial r}\right)^2 + \frac{1}{r^2}\left(\frac{\partial f}{\partial\theta}\right)^2 + 1}} \tag{A7}$$

Then

$$(\hat{Z} \cdot \hat{K}) = \frac{1}{\sqrt{\left(\frac{\partial f}{\partial r}\right)^2 + \frac{1}{r^2}\left(\frac{\partial f}{\partial \theta}\right)^2 + 1}} \tag{A8}$$

And substitution of equation (A8) into (A1)

$$A = \int_{\theta}\int_{r} \sqrt{\left(\frac{\partial f}{\partial r}\right)^2 + \frac{1}{r^2}\left(\frac{\partial f}{\partial \theta}\right)^2 + 1}\ r\, dr\, d\theta \tag{A9}$$

Equation (A9) is true for any arbitrary surface and can now be specified to the geometry of the Centaur liquid-hydrogen tank in which we use a spherical control surface surrounding the outlet line and wish to determine the surface area of that surface.

Now consider the origin of the spherical control surface to be located in the base plane (r, θ) of the Centaur liquid-hydrogen tank along a line drawn from the coordinate origin of the ellipsoidal bulkhead through the centerline of the vertical section of the side outlet at that point where the cylindrical tank sidewall intersects the line. (See fig. 10.) The radius of the spherical control surface is taken to be h_0, and the equation to describe the total spherical surface in cylindrical coordinates is

$$r^2 + Z^2 = h_0^2 \tag{A10}$$

from which

$$f = \sqrt{h_0^2 - r^2} \tag{A11}$$

After taking the appropriate derivatives of (A11) and substituting into (A9), we finally obtain

$$A = \iint_{\theta} \iint_{r} \frac{r\, dr\, d\theta}{\sqrt{1 - \left(\frac{r}{h_0}\right)^2}} \tag{A12}$$

All that remains is to establish the limits of integration in the r-θ plane.

Consider equation (A12) written in the following form:

$$A = 2 \int_{\theta_{min}}^{\pi/2} \int_{0}^{r_m(\theta)} \frac{r\, dr\, d\theta}{\sqrt{1 - \left(\frac{r}{h_0}\right)^2}} \tag{A13}$$

Performing the integration over r yields

$$A = 2h_0^2 \int_{\theta_{min}}^{\pi/2} \left[1 - \sqrt{1 - \left(\frac{r_m}{h_0}\right)^2}\right] d\theta \tag{A14}$$

While it is conceivable that the function $r_m(\theta)$ could be determined analytically, Klavins (ref. 9) approximates the radical in equation (A14) by a quadratic in θ, that is,

$$\sqrt{1 - \left(\frac{r_m}{h_0}\right)^2} \doteq u(\theta) = K_1 + K_2\theta + K_3\theta^2 \tag{A15}$$

With the constants to be evaluated from the conditions

$$u(\theta_{min}) = \frac{h_0}{2a}$$

$$u\left(\frac{\pi}{2}\right) = \sqrt{1 - \left(\frac{d}{h_0}\right)^2} \tag{A16}$$

$$u'\left(\frac{\pi}{2}\right) = 0$$

where the prime denotes differentiation with respect to θ and

$$\frac{d}{h_0} = \frac{\sqrt{1 + \left(\frac{h_0}{b}\right)\left(\frac{a^2}{b^2} - 1\right)} - 1}{\left(\frac{h_0}{a}\right)\left(\frac{a^2}{b^2} - 1\right)}$$

If we now let $\theta_{min} \rightarrow 0$, the constants K_1, K_2, and K_3 can be evaluated and substituted into equation (A14), which, after integration, gives

$$A = \pi h_0^2 \left\{ 1 - \frac{h_0}{6a} - \frac{2}{3}\left[\sqrt{1 - \left(\frac{d}{h_0}\right)^2}\right] \right\} \tag{A17}$$

which is the area of the control surface for $(h_\infty/b) > 1$.

If the initial liquid level is below the top of the ellipsoidal bulkhead, we would anticipate that the flow would primarily be circumferential around the bulkhead, and we could then use two planar surfaces for control areas. (See fig. 11.) In this case the problem is greatly simplified and we simply perform the integration directly at two equal values of θ on either side of the outlet centerline. The appropriate integral is

$$A = 2 \int_{\sqrt{a^2 - \left(\frac{za}{b}\right)^2}}^{a} \int_0^{h_0} dr\, dz \tag{A18}$$

which can be immediately integrated to yield

$$A = 2ah_0 - ab\left[\frac{h_0}{b}\sqrt{1 - \left(\frac{h_0}{b}\right)^2} + \sin^{-1}\left(\frac{h_0}{b}\right)\right] \tag{A19}$$

which is the desired area of the control surface for $(h_\infty/b) < 1$.

Surface Curvature Function

As stated in reference 9, the proper choice for a surface curvature function is strongly dependent on the magnitude of the acceleration environment and the liquid-solid contact angle. At high Bond numbers it is expected that the liquid-vapor interface will be essentially flat except at the tank wall where the liquid-solid contact angle will be maintained. At low Bond numbers and for near zero static contact angles, the interface is highly curved. As stated previously in the text, Klavins (ref. 9) examines four possible forms for the surface curvature function f, two for $B_0 << 1$ and two for $B_0 >> 1$. We will restrict our discussion to those at high Bond numbers.

In general

$$J = \left(\frac{1}{R_1} + \frac{1}{R_2}\right) \tag{A20}$$

where R_1 and R_2 are the principal local radii of curvature at any point.

We consider first the case in which the initial liquid level is high in the tank (see fig. 12). At points far removed from the dip region, the interface is flat, that is, $R_{1_\infty} = R_{2_\infty} \cong \infty$ and thus

$$J_\infty \approx \left(\frac{1}{\infty} - \frac{1}{\infty}\right) \approx 0 \tag{A21}$$

While immediately at the dip region, we will assume that the dip is symmetric, that is, $R_{1_0} = R_{2_0}$. This will not strictly be true because of the curvature of the tank walls. Klavins (ref. 9) makes the assumption that (neglecting terms of order $(h_\infty - h_0)^2$ and higher)

$$R_{1_0} = R_{2_0} \approx \frac{a^2}{2(h_\infty - h_0)} \tag{A22}$$

Then

$$J_\infty - J_0 = \frac{2}{R_{1_\infty}} - \frac{2}{R_{1_0}} = -\frac{4(h_\infty - h_0)}{a^2} \tag{A23}$$

And making use of equation (A23) in the expression for the surface curvature function f (see eq. (5)) we obtain

$$f \approx \frac{1}{4} \tag{A24}$$

which is the expression for the approximate surface curvature function $(h_\infty/b) > 1$.

In similar fashion we may consider the case in which the liquid level in the tank is below the top of the ellipsoidal bulkhead $((h_\infty/b) < 1)$. (See fig. 13.) Again, at points far removed from the drain, the interface is relatively flat, thus

$$R_{1_\infty} = R_{2_\infty} \approx \infty \tag{A25}$$

which leads to

$$J_\infty = \frac{2}{\infty} = 0 \tag{A26}$$

In this case, immediately above the outlet at the dip region, the liquid-vapor interface is a flat ring which is depressed by an amount $(h_\infty - h_0)$ over a portion of the tank above the outlet. If we further assume that the variation in free-surface height is linear along radial lines eminating from the center of the ellipsoidal bulkhead at any fixed value of θ we may say

$$R_{1_0} = \infty \tag{A27}$$

Also, if we assume that the maximum dip at the free-surface occurs just above the center of the outlet line and further that the depression subtends an angle of approximately 90^{o}, it can be shown that

$$R_{2_0} \approx \frac{a^2}{4(h_\infty - h_0)} \tag{A28}$$

Making use of equations (A25) to (A27), we then arrive at

$$J_\infty - J_0 \approx \frac{2}{R_{1_\infty}} - \frac{1}{R_{1_0}} - \frac{1}{R_{2_0}} = -\frac{4(h_\infty - h_0)}{a^2} \tag{A29}$$

which, when substituted into the expression for the surface curvature function (eq. (5)) gives

$$f = \frac{1}{4} \tag{A30}$$

which is the approximate surface curvature function for $(h_\infty/b) < 1$. It should be noted that this approach differs from that taken by Klavens. His result for $(h_\infty/b) < 1$ was $\pi^2/8$.

REFERENCES

1. Nussle, Ralph C.; Derdul, Joseph D.; and Petrash, Donald A.: Photographic Study of Propellant Outflow from a Cylindrical Tank During Weightlessness. NASA TN D-2572, 1965.

2. Derdul, Joseph D.; Grubb, Lynn S.; and Petrash, Donald A.: Experimental Investigation of Liquid Outflow from Cylindrical Tanks During Weightlessness. NASA TN D-3746, 1966.

3. Abdalla, Kaleel L.; and Berenyi, Steven G.: Vapor Ingestion Phenomenon in Weightlessness. NASA TN D-5210, 1969.

4. Berenyi, Steven G.; and Abdalla, Kaleel L.: Vapor Ingestion Phenomenon in Hemispherically Bottomed Tanks in Normal Gravity and in Weightlessness. NASA TN D-5704, 1970.

5. Berenyi, Steven G.: Effect of Outlet Baffling on Liquid Residuals for Outflow from Cylinders in Weightlessness. NASA TM X-2018, 1970.

6. Symons, Eugene P.: Outlet Baffles - Effect on Liquid Residuals from Zero-Gravity Draining of Hemispherically Ended Cylinders. NASA TM X-2631, 1972.

7. Symons, Eugene P.: Effect of Throttling on Interface Behavior and Liquid Residuals in Weightlessness. NASA TM X-3034, 1974.

8. Lacovic, Raymond F.; and Stofan, Andrew J.: Experimental Investigation of Vapor Ingestion in the Centaur Liquid Hydrogen Tank. NASA TM X-1482, 1968.

9. Klavins, Andrew: Vapor Ingestion in a Cylindrical Tank with a Concave Elliptical Bottom. (LMSC/D386845, Lockheed Missiles and Space Co.; NAS 3-17798.) NASA CR-135007, 1974.

10. Bizzel, G. D.; and Crane, G. E.: Numerical Simulation of Low Gravity Draining. (LMSC-D521581, Lockheed Missiles and Space Co.; NAS 3-17798.) NASA CR-135004, 1976.

TABLE I. - PROPERTIES OF EXPERIMENT LIQUID

[Contact angle with cast acrylic plastic in air, 0°]

Liquid	Surface tension at 20° C, σ, N/cm	Density at 20° C, ρ, g/cm^3	Viscosity at 20° C, μ, g/m·sec	Specific surface tension, β, cm^3/sec^2
Ethanol	22.3×10^{-5}	0.789	1.2×10^{-2}	28.3
Trichloro-fluoroethane	18.6×10^{-5}	1.58	$.7\times10^{-2}$	11.8

TABLE II. - SUMMARY OF DATA

Tank radius, a, cm	Test liquid	Flow rate, Q, cm^3/sec	Weber number, $W = Q_0^2/\pi^2\beta a^3$	Bond number, $B = ga^2/\beta$	$W/(1+B)$	Nondimensional vapor-ingestion height, h_∞/b
7.5	TCTFE[a]	152	0.471	4679	1.0×10^{-4}	0.755
7.5	↓	138.26	.390	4679	8.3×10^{-5}	.736
7.5	↓	95.59	.186	4679	4.0×10^{-5}	.672
4	↓	486	31.8	1331	2.4×10^{-2}	1.519
↓	↓	82.07	.905	↓	6.8×10^{-4}	.932
↓	↓	261	9.16	↓	6.8×10^{-3}	1.174
↓	↓	511	35.09	↓	2.6×10^{-2}	1.537
↓	↓	9.4	.013	↓	9.7×10^{-6}	.493
↓	↓	6.8	.0062	↓	4.7×10^{-6}	.447
15	Ethanol	798.7	.678	7805	8.7×10^{-5}	.823
↓	↓	1965	4.1	↓	5.3×10^{-4}	1.1
↓	↓	1517	2.45	↓	3.0×10^{-4}	.856
↓	↓	996	1.05	↓	1.3×10^{-4}	.847
↓	↓	916	.89	↓	1.1×10^{-4}	.81

[a]Trichlorotrifluoroethane.

TABLE III. - SUMMARY OF RESTART PARAMETERS

Event	Bond number, $B = ga^2/\beta$	Weber number, $W = Q^2/\pi^2\beta a^3$	$\log\left(\frac{W}{1+B}\right)$
Line chill down	514	0.0657	-3.89
Engine cool down	3213	.98	-3.52
Main-engine start	1.98×10^{6}	6.18	-5.50

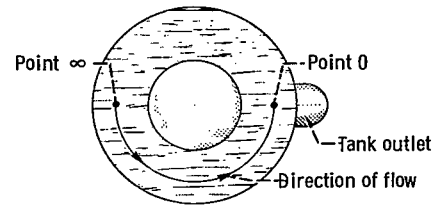

(a) Top view.

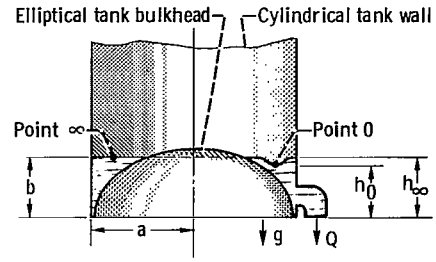

(b) Side view.

Figure 1. - Centaur liquid-hydrogen tank geometry. Definition of terms.

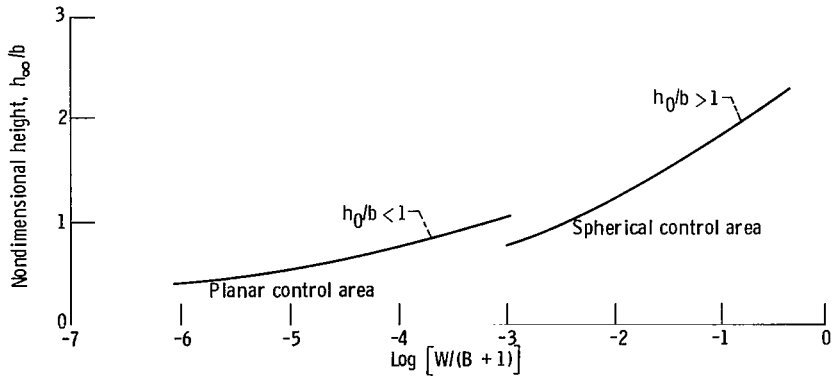

Figure 2. - Calculated vapor ingestion height as function of W/(B + 1) for Bond number of 1000.

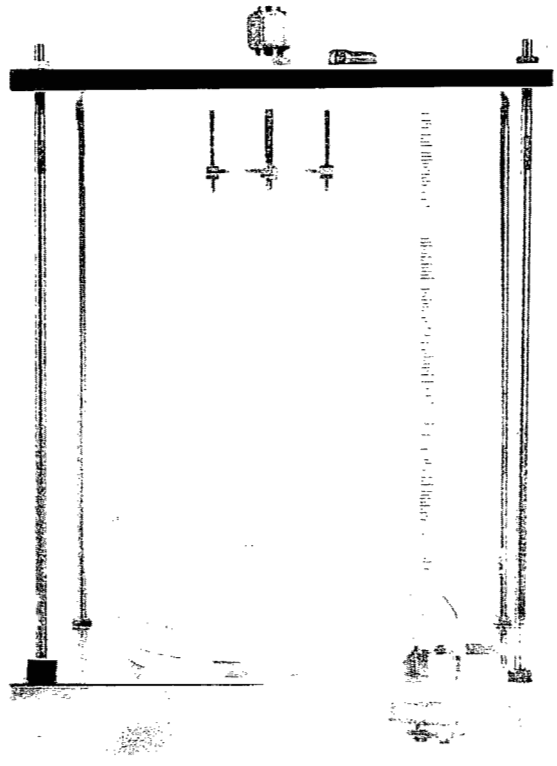

Figure 3. - Experiment tanks.

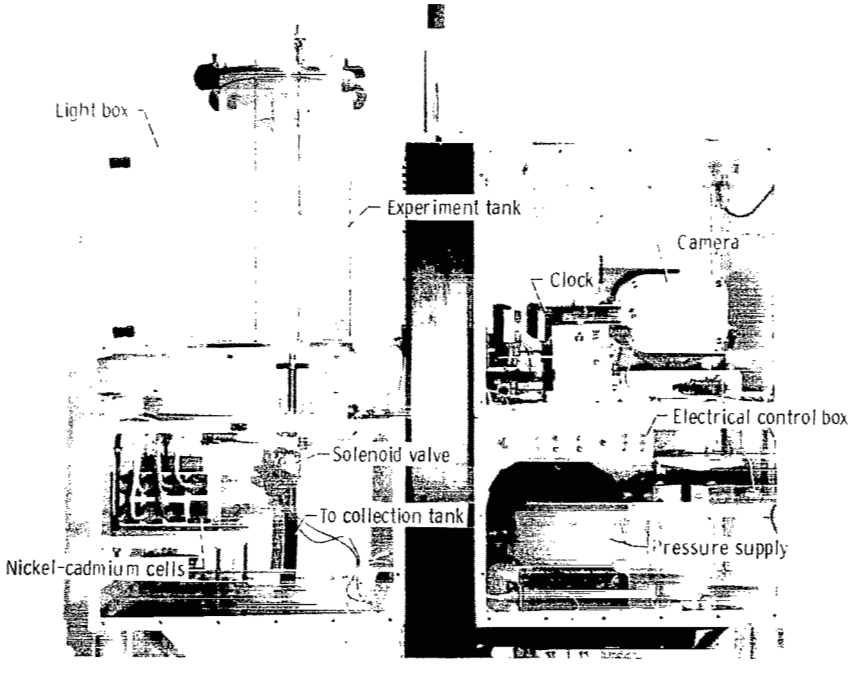

Figure 4. - Experiment package.

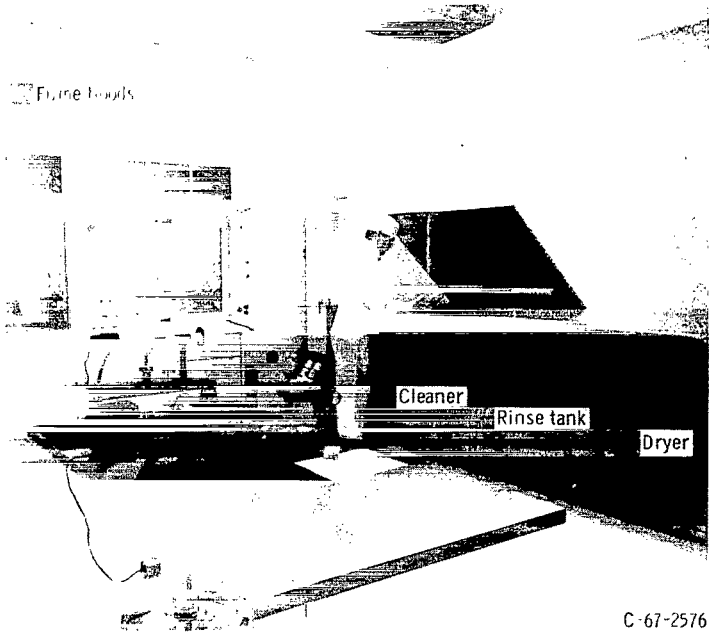

(a) Ultrasonic cleaning system.

(b) Laminar-flow work station.

Figure 5. - Clean room.

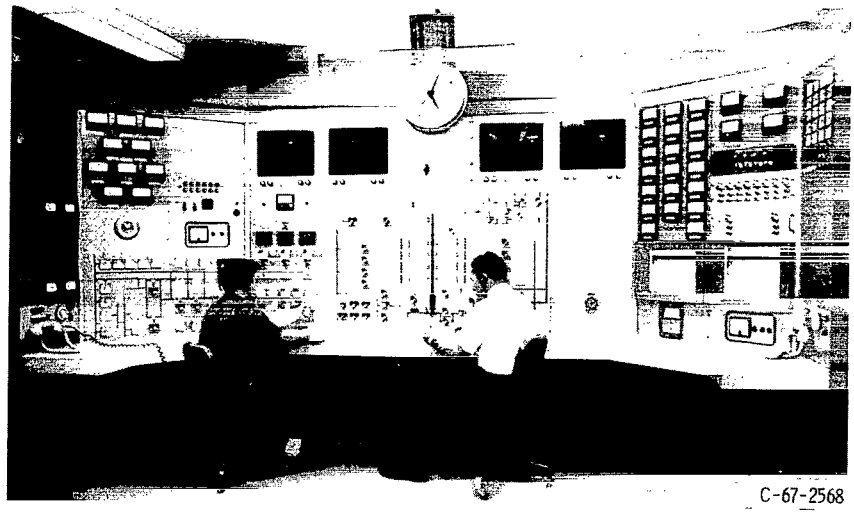

Figure 6. - Control room.

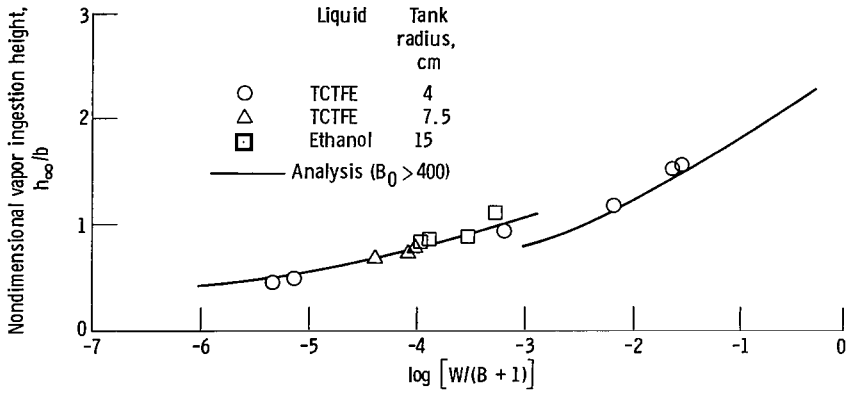

Figure 7. - Comparison of experimental data with analysis. (TCTFE denotes trichlorotrifluoroethane.)

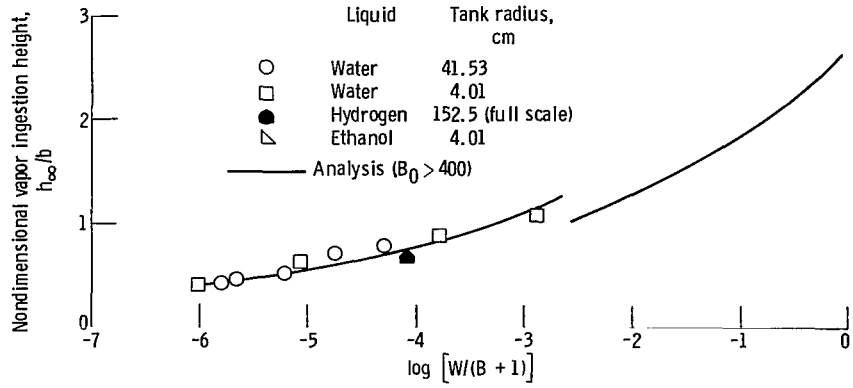

Figure 8. - Comparison of reference 8 data with analysis.

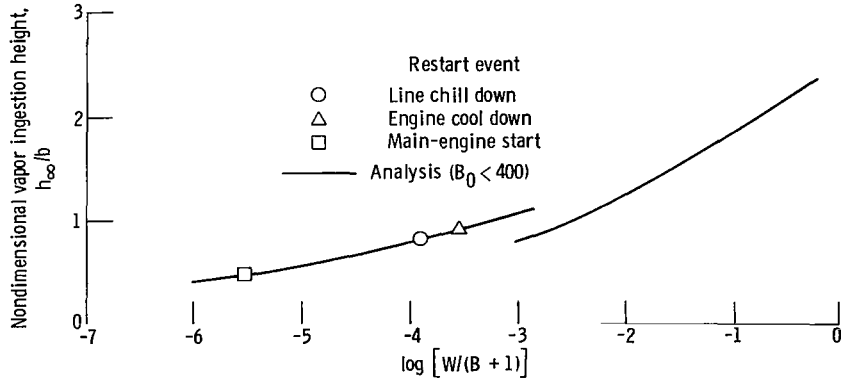

Figure 9. - Predicted vapor ingestion heights during Centaur engine restart.

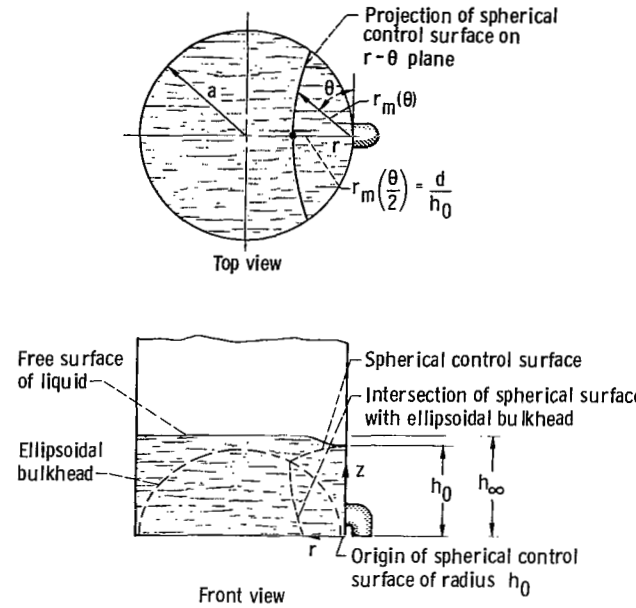

Figure 10. - Approximate control area function ($(h_\infty/b) > 1$).

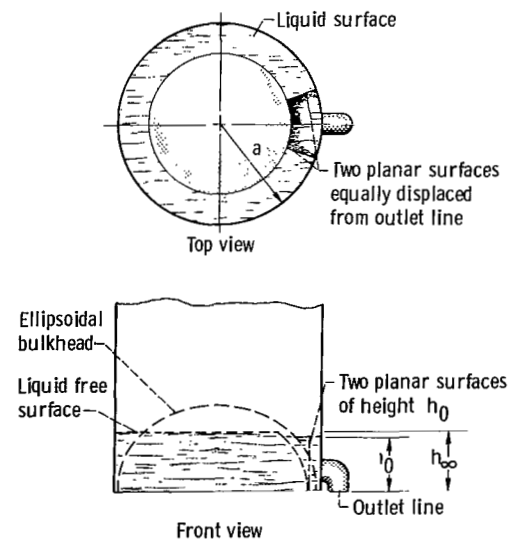

Figure 11. - Approximate control area function ($(h_\infty/b) < 1$).

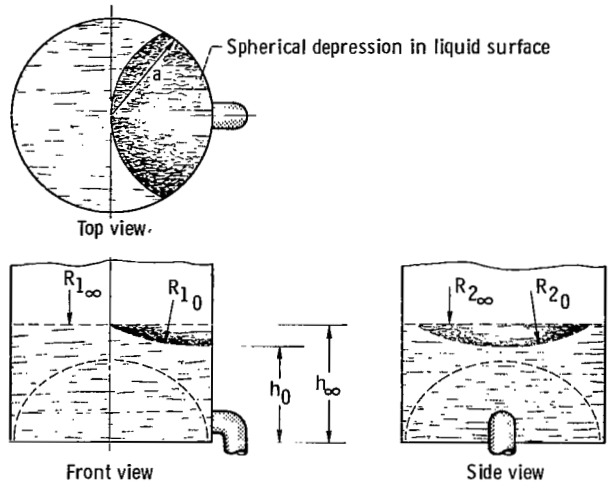

Figure 12. - Approximate surface curvature function $((h_\infty/b) > 1)$.

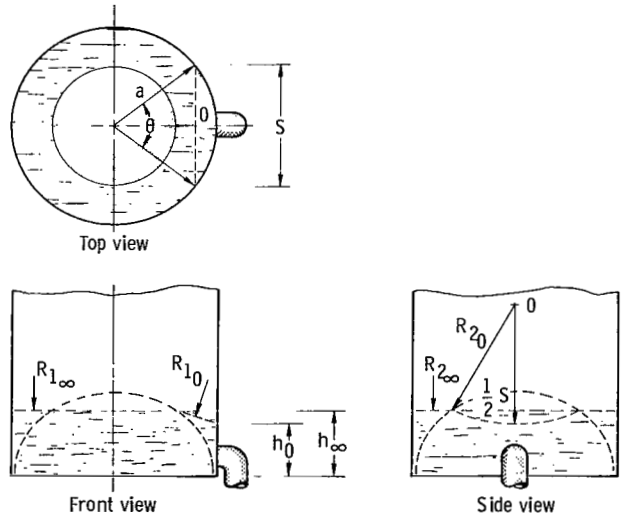

Figure 13. - Approximate surface curvature function $((h_\infty/b) < 1)$.

1. Report No.	2. Government Accession No.	3. Recipient's Catalog No.
NASA TP-1061		

4. Title and Subtitle	5. Report Date
VAPOR INGESTION IN CENTAUR LIQUID-HYDROGEN TANK	October 1977
	6. Performing Organization Code

7. Author(s)	8. Performing Organization Report No.
Eugene P. Symons	E-9234
	10. Work Unit No.
9. Performing Organization Name and Address	491-02
National Aeronautics and Space Administration Lewis Research Center Cleveland, Ohio 44135	11. Contract or Grant No.
	13. Type of Report and Period Covered
12. Sponsoring Agency Name and Address	Technical Paper
National Aeronautics and Space Administration Washington, D.C. 20546	14. Sponsoring Agency Code

15. Supplementary Notes

16. Abstract

An experimental investigation of the vapor-ingestion phenomena in scale models of the Centaur liquid-hydrogen tank was conducted to determine the height of the free surface of the liquid when vapor is initially ingested into the tank outlet. Data are compared with an analysis and, in general, the agreement is very good. Additionally, predictions of minimum liquid levels required in the Centaur liquid-hydrogen tank in order to prevent vapor ingestion when restarting the engines in space and the quantities of liquid remaining in the tank at vapor ingestion during main-engine firing are presented.

17. Key Words (Suggested by Author(s))	18. Distribution Statement
Cryogenic rocket propellants Vapor ingestion Tank draining Suction dip	Unclassified - unlimited STAR Category 34

19. Security Classif. (of this report)	20. Security Classif. (of this page)	21. No. of Pages	22. Price*
Unclassified	Unclassified	30	A03

* For sale by the National Technical Information Service, Springfield, Virginia 22161

National Aeronautics and Space Administration

Washington, D.C.
20546

Official Business
Penalty for Private Use, $300

THIRD-CLASS BULK RATE

Postage and Fees Paid
National Aeronautics and Space Administration
NASA-451

U.S.MAIL

3 1 1U,D, 093077 S00903DS
DEPT OF THE AIR FORCE
AF WEAPONS LABORATORY
ATTN: TECHNICAL LIBRARY (SUL)
KIRTLAND AFB NM 87117

S

NASA

POSTMASTER: If Undeliverable (Section 158 Postal Manual) Do Not Return